Journal of the Korean Ceramic Society (2024) 61:97–103
https://doi.org/10.1007/s43207-023-00350-0

ORIGINAL ARTICLE

Nd composite selective recovery from waste permanent magnet scrap powders by solid-fluorination reaction

Yun-Ho Jin[1,2] · Hee-Seon Kim[1] · Jae-Kyo Yang[1] · Dae-Weon Kim[1] · Dong-Wan Kim[2]

Received: 7 September 2023 / Revised: 13 November 2023 / Accepted: 21 November 2023 / Published online: 14 December 2023

Abstract
This study proposes a novel waste permanent magnet (WPM) recycling technology by avoiding conventional technology that relies on strong acid and developing a feasible process using relatively inexpensive reagents, thereby reducing overall process cost to acceptable levels. $Nd_2Fe_{14}B$ WPMs were transformed into a fluoride/oxide composite material through oxidation/fluorination heat treatment. The phase transition from FeF_3-NdF_3 to Fe_2O_3-NdF_3 composition was performed via heat treatment. The Fe_2O_3-NdF_3 composition is selectively leached using an oxalic acid. It was confirmed that Fe_2O_3 was selectively leached, and NdF_3 was leached at less than 1 wt.% under various leaching conditions. The neodymium fluoride produced using this technology is expected to be applicable to related fields such as Nd smelting flux or catalysts, and this technology is expected to be applied to various materials containing Fe.

Keywords Permanent magnet · Phase transition · Oxalic acid · Selective leaching · Recovery

1 Introduction

Nd permanent magnets are among the strongest permanent magnets with the highest magnetic field, in high demand in devices that require strong magnetic fields while remaining lightweight and compact, such as microphone speakers, computer hard drives, electric vehicle motors, wind turbine generators, and medical MRI machines. Nd recovery is essential to stabilize the supply and demand of the rare earth element, and various methods are being explored [1–4]. The average annual growth rate of Nd, which is used in various applications, exceeds 22.5%.

There are few commercial methods to produce Nd metal as molten salt or electrodeposition. Considering molten salt, NdF_3-LiF flux or other halides/chlorides are used as electrolyte systems [5, 6]. Because Nd permanent magnets are very fragile, a large amount of scrap is generated during the magnet manufacturing process, and this process scrap is known to be more than 30%. Most of Nd, the key element of Nd permanent magnets, is buried in China. Therefore, Nd recycling technology is very important.

This study presents a novel method for Nd recovery as a compound from waste permanent magnets (WPMs) using NdF_3 synthesis. Although little is known about NdF_3 solubility, a chemically stable material was produced. The conventional Nd permanent magnet recycling process used strong acid solutions for Fe and Nd selective separation, however, due to environmental concerns, a relatively mild and weak acidic technology for Nd selective recovery is required.

2 Methods

The fluorination heat treatment and selective leaching overall flowchart for WPMs is shown in Fig. 1.

2.1 Materials

The WPM was obtained from the manufacturer and the powder was confirmed to be $Nd_2Fe_{14}B$ permanent magnet through X-ray diffraction (XRD) (X-ray diffractometer, XRD-6100, Shimadzu, Japan) analysis in Fig. S1. The particle size was evaluated by particle size analyzer (PSA,

✉ Dae-Weon Kim
mdsimul@iae.re.kr

✉ Dong-Wan Kim
dwkim1@korea.ac.kr

[1] Center for Advanced Materials and Processing, Institute for Advanced Engineering, Yong In 17180, South Korea

[2] School of Civil, Environmental, and Architectural Engineering, Korea University, Seoul 02841, South Korea

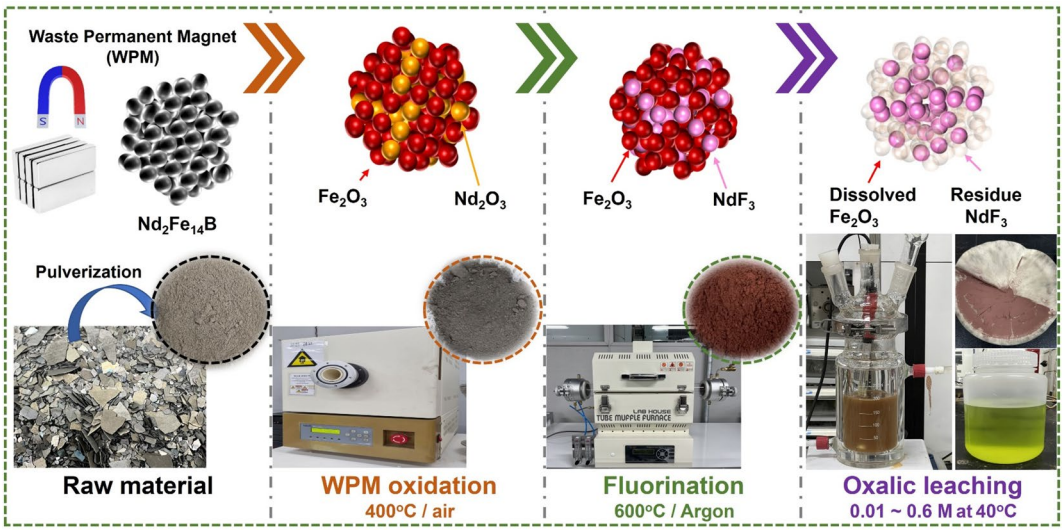

Fig. 1 Overall flowchart

Bluewave, Microtrac, Germany) in Fig. S2. The composition of WPM was analyzed by X-ray fluorescence (XRF) (X-ray fluorescence, XRF-1800, Shimadzu, Japan) in Table S1. The WPM powder was heat treated at 400 °C and 600 °C in air for oxidation from the metal phase, and XRD analysis was conducted on the powders, respectively, followed by phase transformation from oxide to fluorination. The oxidized powders were mixed with ammonium bifluoride (ABF). (ABF, NH_4HF_2, Sigma-aldrich, 98%) The ABF was mixed with mortar for 30 min.

2.1.1 Commercial powders used in fluorination heat treatment

Commercial powder was used to study the oxidized WPM material composition fluorination phase transformation. We experimented with fluorination reaction commercial Fe_2O_3 (Sigma-aldrich, 99%) and Nd_2O_3 (Sigma-aldrich, 99%), respectively. Considering Fe_2O_3, the Fe_2O_3 to FeF_3 phase transition was observed through heat treatment at 350–600 °C at a molar ratio of 1:6.

Commercial Nd_2O_3 was also subjected to molar ratio heat treatment with ABF at a 1:4–1:6 ratio. The Nd_2O_3 fluorination heat treatment was performed at 600 °C.

2.1.2 WPM fluorination heat treatment

Fluorination heat treatment using commercial powders was performed on the WPM. The WPM powder was heat treated at 400 °C in air, thereafter, the ABF and oxidized WPM was mixed at a molar ratio of 1:6, and heat treatment was performed at 600 °C in an argon flow with low vacuum.

2.2 Leaching procedure

2.2.1 Commercial NdF_3 solubility in various acid/base solutions

NdF_3 solubility (Alfa-aesar, 99%) was evaluated using 10 M NH_4OH, 4 M H_2SO_4, 4 M HNO_3, 10 M HNO_3, 4 M HCl, and 6 M HCl. The leaching tests were carried out at 25 °C, the solutions were maintained for more than 24 h, and the leached solution was analyzed by inductively coupled plasma (ICP) (iCAP Pro XP, ThermoFisher). The pulp density was set at 5 g/100 mL and RPM was fixed at 300.

2.2.2 Fluorinated WPM oxalic acid leaching study

WPM powders were heat treated for fluorination at 600 °C, the powder immersed in 0.01–0.6 M oxalic acid solution at 40–50 °C. The pulp density was set at 1%, and RPM was fixed at 300. The leaching procedure was conducted for 8 h, and the leached solution ICP analysis results and residual XRD analysis were conducted after reaction completion.

2.3 Thermodynamic calculations

All compositions were characterized by their Gibbs free energy of formation value, which quantify the energy released or consumed during transformation of a phase from its constituent elements in their standard state. The HSC Chemistry software 10.0, includes databases and various modules providing different types of chemical/thermodynamic calculations. The enthalpy and entropy values were available in their databases. We used the 'Reaction equation'

module for calculation of changes of Gibbs free energy for various calcination temperatures" and "Equilibrium calculations" module for assumed that practical way to observe the effects of process variable, according to the calcination temperature and amounts of raw materials.

3 Results and discussion

3.1 Oxidation and fluorination heat treatment

The pulverized WPM powder XRD analysis established that it was an $Nd_2Fe_{14}B$ permanent magnet. The particle size was confirmed to be approximately 1 μm. The WPM powder was subjected to oxidation heat treatment at 400 °C and 600 °C. The XRD analysis after heat treatment at 400 °C established that the main materials were Fe_2O_3 and Nd_2O_3 in Fig. 2.

XRD was used to identify the powder phases. The peaks observed at 2 theta = 24.14°, 33.15°, and 35.63° were identified as Fe_2O_3 (JCPDS #79–1741). Due to the relatively low amount of neodymium in the permanent magnet, the Nd_2O_3 minor peaks (JCPDS #21–0579) were observed at 2 theta = 27.85°, 46.30°, and 54.93°, detected via XRD. The 400 °C oxidation heat treatment results showed only Fe_2O_3 and Nd_2O_3, with no observation of the high-temperature $FeNdO_3$ stable phase. In the 600 °C oxidation heat treatment, the observed $FeNdO_3$ was identified at 2 theta = 22.84°, 32.54°, and 46.53° ($FeNdO_3$, JCPDS #25–1149). Reactivity thermodynamic calculations with ABF were performed using HSC Chemistry 10 for the Nd_2O_3 and Fe_2O_3 produced through a 400 °C oxidation heat treatment, as well as for the $NdFeO_3$ produced through a 600 °C oxidation heat treatment. The predicted reaction equations and their corresponding ΔG values are as follows:

(i) $Fe_2O_3 + Nd_2O_3 + 6NH_4HF_2 = 2NdF_3 + 2FeF_3 + 6NH_3(g) + 6H_2O(g)$

ΔG = −785.46 kJ at 400 °C, ΔG = −1,046.19 kJ at 600 °C in reaction (i) in Table S2.

(ii) $2NdFeO_3 + 6NH_4HF_2 = 2NdF_3 + 2FeF_3 + 6NH_3(g) + 6H_2O(g)$

ΔG = −172.39 kJ at 400 °C, ΔG = −237.302 kJ at 600 °C in reaction (ii) Table S2.

The thermodynamics calculation indicated that oxidation heat treatment at 400 °C would result in more spontaneous reactions, as well as a lower energy cost due to the facile phase transition at lower temperatures. We confirmed that both Fe_2O_3 and Nd_2O_3 were oxidized, respectively, whereafter we carried out a fluorination heat treatment study using commercial Fe_2O_3.

Heat treatment was performed at a 1:6 molar ratio with ABF at 350–600 °C. After heat treatment, XRD powder analysis was performed as shown in Fig. 3. At 350 °C, we confirmed that Fe_2O_3 was phase transformed to single-phase $FeF_3 \cdot 0.33H_2O$ (JCPDS #76–1262). It was identified at 2 theta = 13.79°, 23.62°, and 27.80°. The powders showed that $FeF_3 \cdot 0.33H_2O$ remained at 385 °C, however, crystallinity was weaker than that at 350 °C. We observed phase transform to FeF_3 with minor amounts of FeF_2 at 400 °C. It was determined that 2 theta = 23.84°, 33.42°, and 40.18°. (JCPDS #88–2023). We conducted fluorination heat treatment at 600 °C, in which the powders transformed to single-phase Fe_2O_3. It appears that the powders re-oxidized to Fe_2O_3 at high temperatures of above 400 °C [7].

(iii) $NH_4FeF_4 + H_2O + NH_3 + H_2 < 350$ °C

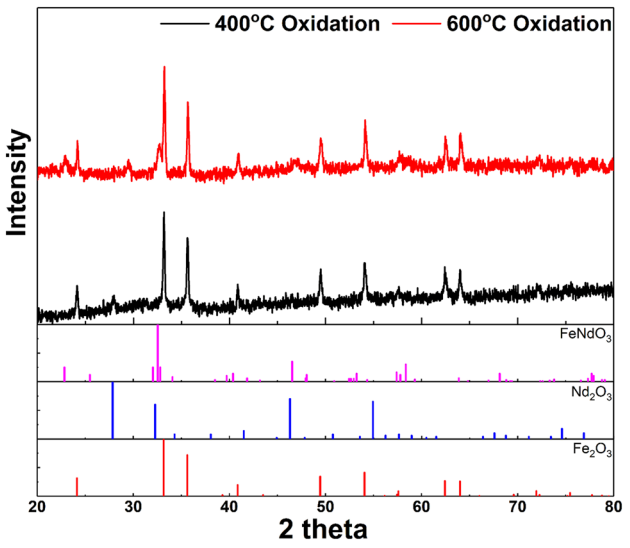

Fig. 2 Waste permanent magnet (WPM) oxidation and fluorination X-ray diffraction (XRD) patterns at 400 °C and 600 °C

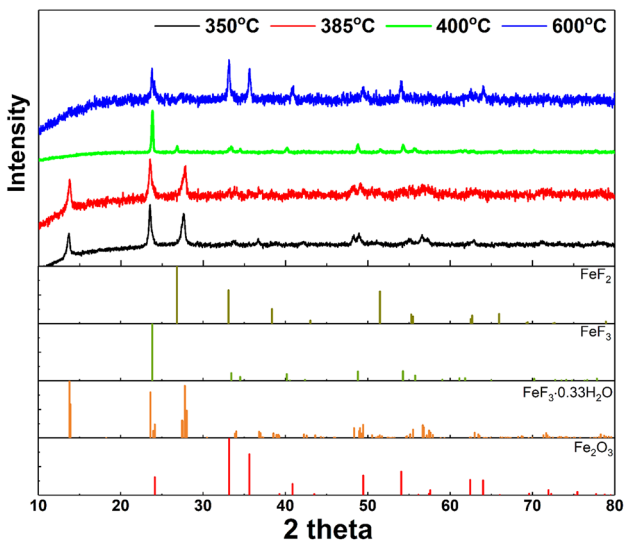

Fig. 3 Commercial Fe_2O_3 fluorination X-ray diffraction (XRD) patterns at various temperatures

(iv) FeF_3 0.33 H_2O + evaporated gas < 400 °C

(v) FeF_3 + dehydration gas (nH_2O) → Fe_2O_3 + HF(g)

Based on the above-presumed reaction equations (iii) ~ (v), thermodynamic calculations were performed for FeF_3 re-oxidation.

(vi) $2FeF_3 + 3H_2O(g) = Fe_2O_3 + 6HF(g)$

Assuming a reaction of (vi), the Gibbs free energy has a negative value above 500 °C (ΔG = −16.97 kJ) in Table S3, calculated as ΔG = −49.41 kJ at 600 °C. The ΔG value increased proportionally as the temperature increased. The above reaction was calculated as a spontaneous reaction as the temperature increased [8, 9]. When FeF_3 reacted with evaporated O_2 was calculated, ΔG was also negative. FeF_3 was not stable with the oxygen reaction in Table S4.

To elucidate the Nd_2O_3 reaction with ABF, commercial Nd_2O_3 was used with various ABF molar ratios. The reaction temperature was maintained at 600 °C. The XRD patterns are shown in Fig. S3. We confirmed that single-phase NdF_3 was observed above a molar ratio of 1:6. The diffraction patterns matched NdF_3 (JCPDS #09–0416) in Fig. S3., and minor NdF_2 (JCPDS #33–0934) peaks are observed. Previously, the re-oxidation by hydration regarding FeF_3 could be confirmed through thermodynamic calculation and actual experiments for the high-temperature reaction. Considering NdF_3, the thermodynamic calculation was conducted as NdF_3 reacted with oxygen and hydration. It was confirmed that NdF_3 is stable against oxygen or hydration at high temperatures. The reaction calculation showed that when the NdF_3 reacted with $H_2O_{(g)}$, the ΔG value was 146.15 kJ at 1000 °C (Table S5). Additionally, when reacting with oxygen, the ΔG value calculated positive at 1000 °C (Table S6).

From the reaction results of commercial Fe_2O_3 and Nd_2O_3 with ABF, we confirmed that Fe_2O_3 transformed to FeF_3 below 400 °C, however, it re-oxidized to Fe_2O_3 at 600 °C. To confirm the actual WPM powder reaction results, the WPM powder oxidized at 400 °C was subjected to fluorination heat treatment at 400 °C and 600 °C, respectively. Consequently, XRD results of the powder obtained after heat treatment by solid mixing with ABF at 400 °C confirmed FeF_3 at 2 theta = 23.83° and 54.29°, respectively. (JCPDS #75–0451) The main phase was confirmed as NdF_3 and some Fe_2O_3 was also observed in Fig. 4.

It was established that FeF_3 completely disappeared during the fluorination heat treatment at 600 °C, and only two phases of Fe_2O_3 and NdF_3 were observed. When the FeF_3 reacts with ABF at high temperatures of 600 °C or above, it can be determined that both commercial and WPM powders phase transition from FeF_3 to Fe_2O_3. Higher NdF_3 and Fe_2O_3 crystallinity was confirmed in the 600 °C fluorination heat treatment. We performed thermodynamic calculations of the oxidized WPM powder fluorination. The total amount of each component generated can be calculated using Fig. S4(a). Correlation between thermodynamic calculations and the actual experiments of selective specific material such as Nd_2O_3, Fe_2O_3, NdF_3, FeF_3 and $H_2O_{(g)}$ were confirmed as shown in Fig. S4(b).

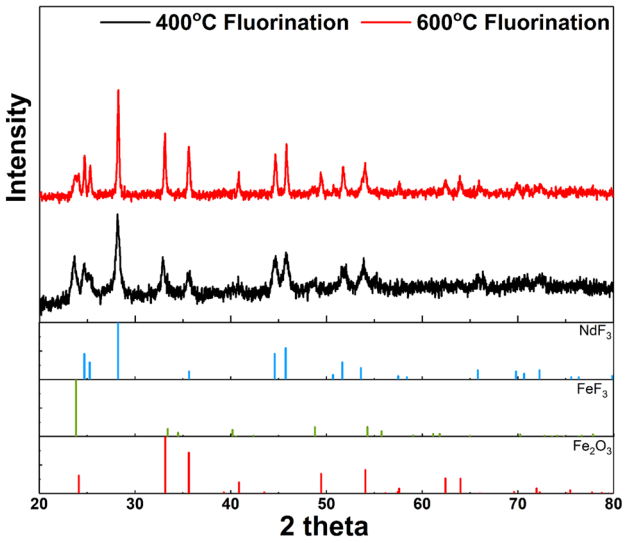

Fig. 4 Oxidized-WPM fluorination X-ray diffraction (XRD) patterns at 400 °C and 600 °C

As a result of the SEM analysis, the WPM powder was observed at approximately 1 μm as shown in Fig. S5(a). Smaller particles were observed, which are believed to be due to surface oxidation from heat-generated friction created during the metal powder crushing/grinding process. It was confirmed that plate-like particles were entangled around the surface with a surface size of several nanometers.

In the powder after the oxidation heat treatment process at 400 °C, some oxidized particles were observed in Fig. S5(b). The primary particles were nano-sized, however, secondary particles sizes were observed at a maximum of 10 μm or greater.

3.2 Selective leaching

Little is known about NdF_3 solubility in acid or base solutions [10]. Several acid/base solutions were prepared, and each concentration was set and maintained for more than a day to observe the leaching rate. The final pH of 10 M NH_4OH was measured as 12.31 and NdF_3 did not dissolve at all. The final pH of 4 M H_2SO_4 was measured as -1.44, and the Nd concentration was analyzed in the solution at 79.5 ppm. The final pH of both the 4 M and 10 M nitric acids was measured as −1.35, and the Nd concentration was 30.9 ppm. Regarding 4 M HCl, the final pH was measured as −0.15, and Nd was confirmed to have similar behavior to sulfuric acid at 80.6 ppm, however, this leaching rate was negligible. When leaching was attempted using 6 M HCl, it was performed for a maximum of 2 d, and NdF_3

solubility was approximately 0.2%. It was confirmed that NdF_3 is highly stable in the commonly used acidic solution. However, FeF_3 is known to exist in various phases such as a number of hydrates and it is known that it could be leached into water and acid when it consists of hydrate [11].

Based on the pure NdF_3 leaching results, using the Fe_2O_3 and NdF_3 composite phase from fluorination heat treatment at 600 °C, only Fe_2O_3 could be selectively leached and separated. Fe_2O_3 selective leaching was attempted using oxalic acid. Oxalic acid is known as a weak acid with an acidity of 1.25 or 4.14 depending on the dissolved ionic form. There has been scant research on highly selective leaching techniques using a weak acid [12, 13]. This technology uses a weak oxalic acid, in contrast to most techniques which use strong acids or expensive ionic liquids, which can reduce the environmental burden and process costs. Selective Fe_2O_3 leaching with oxalic acid is well known [14–16], also especially the oxalic acid is preferable and more effective leaching agents such as citric, ascorbic, gluconic or malic acid for leaching out of iron oxide [17, 18]. There are several oxalic acid-assisted Nd magnet recycling studies [19, 20].

The overall Fe_2O_3 leaching rate in fluorinated-WPM powders under various leaching conditions is shown in Fig. 5, and that of rare earth material (Nd) in fluorinated-WPM powders under the same conditions is shown in Fig. 6.

During the after 2 h, the leaching rate exceeded 50% in most leaching conditions (except for 0.01 M oxalic acid). It was confirmed that the leaching rate increased continuously over time, and the 0.6 M Fe leaching rate approached 97.8% at 40 °C and 96.9% at 50 °C after 8 h. The 0.3 M leaching rate was approached below 80% even after 8 h. (71.8% after 4 h, 72.7% after 8 h, respectively) We considered the reaction time, it was expected that the leaching rate did not increase for 4 h. The reason for the negligible Fe leaching rate according to reaction time is that we considered to have occurred from re-precipitation as Fe oxalate during Fe_2O_3 leaching in oxalic acid. This was clearly confirmed when XRD analysis of the residue was performed as shown in Fig. 7. Optimal leaching conditions were confirmed by using a minimum amount of oxalic acid to minimize energy use and resources during leaching. Under experimental conditions, only Fe oxide could be selectively leached using a concentration of 0.08 M oxalic acid. Consequently, the leaching rate using 0.05 M oxalic acid was less than 60% within 8 h, and in the case of 0.01 M oxalic acid, the leaching rate was less than 20%.

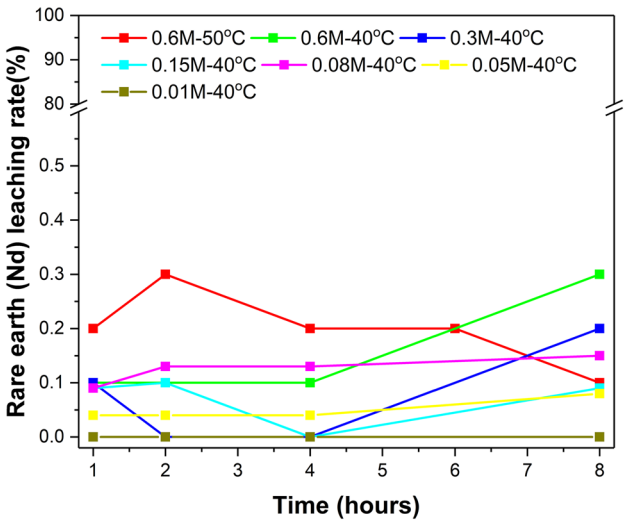

Fig. 6 Nd leaching rate in fluorinated-WPM powders under various leaching conditions

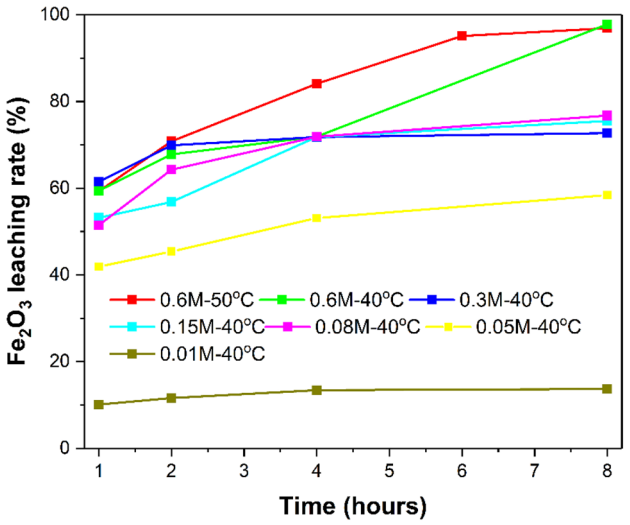

Fig. 5 Fe_2O_3 leaching rate in fluorinated-WPM powders under various leaching conditions

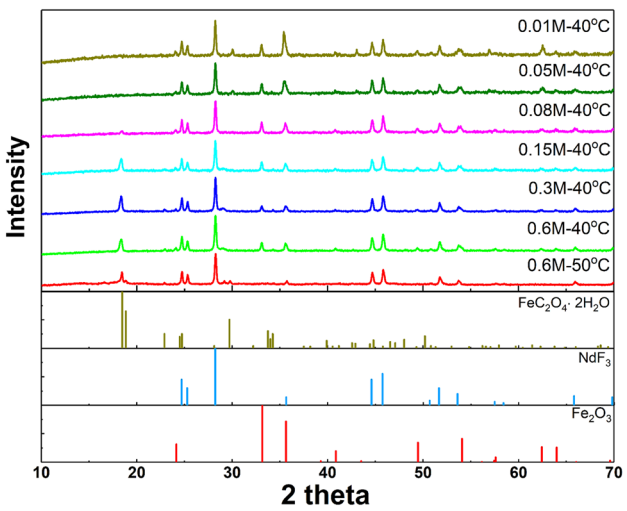

Fig. 7 Residue X-ray diffraction (XRD) patterns after oxalic acid leaching

It can be expected that the oxalic acid concentration for leaching Fe_2O_3 in the powder was insufficient. This result contrasted from a Fe leaching rate of 70% or greater at a concentration of 0.08 M oxalic acid. As a result of selective leaching with oxalic acid through fluorination heat treatment, the rare earth (Nd) material leaching rate was suppressed to a maximum of 0.3%, confirming selective leaching behavior. A maximum Nd leaching rate of 0.3% was obtained using 0.6 M oxalic acid, where Fe_2O_3 was leached out very selectively, and it was confirmed that NdF_3 material has a high chemical resistance to both weak acid/strong acid/base solutions. Rare earth leaching data for Nd, Dy and Pr are shown in Table 1.

It was confirmed that the main peaks were observed as Fe_2O_3 almost disappeared as the residue powder was heated up to 600 °C for fluorination before leaching as shown in Fig. 7. In particular, the Fe_2O_3 main peaks at 2 theta = 33.15°, and 35.63°, were not observed using 0.6 M at 50 °C. It was observed that Fe_2O_3 was completely leached by oxalic acid, and $FeC_2O_4 \cdot 2H_2O$ (JCPDS #23–0293) was detected from XRD analysis of the residue after the Fe ions in the leachate were reduced for 8 h or more. It was shown that 2 theta = 18.46°, 18.86°, 29.71°, and 33.74° coincides with the main peaks, respectively. Fe oxalate dihydrate is composed of two hydrates, however, its solubility in water is known to be very low at 0.097 g/100 ml. Therefore, it was confirmed that it was not dissolved in an aqueous solution of 0.6 M oxalic acid and re-precipitated during the leaching process. It was confirmed that the amount of Fe oxalate decreased as the oxalic acid concentration for leaching decreased. Fe oxalate hydrate was hardly observed at 0.08 M and not observed at 0.05–0.01 M. This is expected to have insufficient driving force for Fe oxalate to be precipitated while Fe oxide is leached by oxalic acid. Therefore, it is considered that pure NdF_3 can be recovered by selectively leaching sufficient Fe_2O_3 and separating it from NdF_3 during multi-stage leaching at a concentration of 0.05 M.

Table 1 Rare earth (Nd, Dy and Pr) leaching rate according to leaching conditions

Oxalic acid concentration and Temperature/Time	Nd (%)	Dy (%)	Pr (%)
0.01 M at 40 °C/8 h	0	0.05	0.02
0.05 M at 40 °C/8 h	0.08	0.41	0.13
0.08 M at 40 °C/8 h	0.15	0.21	0.18
0.15 M at 40 °C/8 h	0.09	0.14	0.09
0.3 M at 40 °C/8 h	0.2	0.3	0.3
0.6 M at 40 °C/8 h	0.3	0.4	0.3
0.6 M at 50 °C/8 h	0.1	0.2	0.1

4 Conclusion

To recycle WPMs, we developed a technology that can replace the existing strong acid-based technology such as sulfuric acid/hydrochloric acid. By inducing a solid-state reaction with solid ABF, a fluoride/oxide complex was prepared, and the prepared Fe oxide was leached with a weak acid, oxalic acid, to obtain an NdF_3 and Fe ion solution. It could be recovered together in the form of Fe oxalate according to the reaction time control. It has the advantage of significantly lowering the process cost by eliminating the acid treatment burden due to the strong acid use, and not only does it have no elements harmful to the environment, the recovered NdF_3 can be used as a flux to reduce Nd_2O_3, or used as a catalyst.

Supplementary Information The online version contains supplementary material available at https://doi.org/10.1007/s43207-023-00350-0.

Acknowledgements This work was supported by the Korea Evaluation Institute of Industrial Technology (KEIT), which is funded by the Ministry of Trade, Industry, and Energy, Republic of Korea (Project No. 20015769). This research was supported by Basic Science Research Program through the National Research Foundation of Korea (NRF) funded by the Ministry of Education (2020R1A6A1A03045059). We thank the Korea Basic Science Institute for the technical support.

Funding This research did not receive any specific grant from funding agencies in the public, commercial, or not-for-profit sectors.

Data availability The authors declare that the data supporting the findings of this study are available within the paper, its supplementary information file.

Declarations

Conflict of interest There are no conflicts of interest to declare that are relevant to the content of this article.

References

1. T. Itakura, R. Sasai, H. Itoh, Resource recovery from Nd-Fe-B sintered magnet by hydrothermal treatment. J. Alloys Compd. **408**, 1382–1385 (2006). https://doi.org/10.1016/j.jallcom.2005.04.088
2. C.-H. Lee, Y.-J. Chen, C.-H. Liao, S. R. Popuri, S.-L. Tsai, C.-E. Hung, Selective leaching process for neodymium recovery from scrap Nd-Fe-B magnet. Metall. Mater. Trans. A Phys. Metall. Mater. Sci. **44**, 5825–5833 (2013). https://doi.org/10.1007/s11661-013-1924-3
3. T.H. Okabe, O. Takeda, K. Fukuda, Y. Umetsu, Direct extraction and recovery of neodymium metal from magnet scrap. Mater. Trans. **44**(4), 798–801 (2003). https://doi.org/10.2320/matertrans.44.798
4. S. Li, Z. Cui, W. Li, D. Wang, Z. Wang, Technical actuality and prospect of NdFeB waste recycling. Mater. Rep **35**, 3001–3009 (2021)

5. C. Huang, X. Liu, Y. Gao, S. Liu, B. Li, Cathodic processes of neodymium(III) in LiF-NdF_3-Nd_2O_3 melts. Faraday Discuss. **190**, 339–349 (2016). https://doi.org/10.1039/c6fd00014B
6. E. Stefanidaki, C. Hasiotis, C. Kontoyannis, Electrodeposition of neodymium from LiF-NdF–3-Nd_2O_3 melts. Electrochim. Acta **46**(17), 2665–2670 (2001). https://doi.org/10.1016/S0013-4686(01)00489-3
7. J. Chun, C. Jo, S. Sahgong, M.G. Kim, E. Lim, D.H. Kim, J. Hwang, E. Kang, K.A. Ryu, Y.S. Jung, Y. Kim, J. Lee, Ammonium fluoride mediated synthesis of anhydrous metal fluoride-mesoporous carbon nanocomposites for high-performance lithium ion battery cathodes. ACS Appl. Mater. Interfaces **8**(51), 35180–35190 (2016). https://doi.org/10.1021/acsami.6b10641
8. B. Kozekanan, A. Moradkhani, H. Baharvandi, Thermodynamic and phase analysis of SiC-nano/microB4C-C composites produced by pressureless sintering method. J. Korean Ceram. Soc. **59**, 180–192 (2022). https://doi.org/10.1007/s43207-021-00173-x
9. H. Bae, Y. Shin, L. Mathur, Defect chemistry of p-type perovskite oxide La0.2Sr0.8FeO3-δ: a combined experimental and computational study. J. Korean Ceram. Soc. **59**, 876–888 (2022). https://doi.org/10.1007/s43207-022-00237-6
10. E.P. Lokshin, O. Tareeva, Solubility of YF_3, CeF_3, PrF_3, NdF_3, and DyF_3 in solutions containing sulfuric and phosphoric acids. Russ. J. Inorg. Chem. **52**(12), 1830–1834 (2007). https://doi.org/10.1134/S0036023607120042
11. K.M. Österdahl, Å.C. Rasmuson, Solubility of β-$FeF_3{\cdot}3H_2O$ in mixtures of nitric and hydrofluoric acid. J. Chem. Eng. Data **51**(1), 223–229 (2006). https://doi.org/10.1021/je050347n
12. M. Gergoric, A. Barrier, T. Retegan, Recovery of rare-earth elements from neodymium magnet waste using glycolic, maleic, and ascorbic acids followed by solvent extraction. J. Sustain. Metall. **5**, 85–96 (2019). https://doi.org/10.1007/s40831-018-0200-6
13. G. Reisdörfer, D. Bertuol, E.H. Tanabe, Recovery of neodymium from the magnets of hard disk drives using organic acids. Miner. Eng. **143**, 105938 (2019). https://doi.org/10.1016/j.mineng.2019.105938
14. S.O. Lee, T. Tran, B.H. Jung, S.J. Kim, M.J. Kim, Dissolution of iron oxide using oxalic acid. Hydrometallurgy **87**(3–4), 91–99 (2007). https://doi.org/10.1016/j.hydromet.2007.02.005
15. C. Nwoye, Model for evaluation of the concentration of dissolved phosphorus during leaching of iron oxide ore in oxalic acid solution. JMMCE **8**(3), 181–188 (2009). https://doi.org/10.4236/jmmce.2009.83016
16. R. Salmimies, M. Mannila, J. Kallas, A. Häkkinen, Acidic dissolution of hematite: Kinetic and thermodynamic investigations with oxalic acid. Int. J. Miner. Process. **110**, 121–125 (2012). https://doi.org/10.1016/j.minpro.2012.04.001
17. V. Ambikadevi, M. Lalithambika, Effect of organic acids on ferric iron removal from iron-stained kaolinite. Appl. Clay Sci. **16**, 133–145 (2000). https://doi.org/10.1016/S0169-1317(99)00038-1
18. V. Arslan, A study on the dissolution kinetics of iron oxide leaching from clays by oxalic acid. Physicochem. Probl. Miner. Process, **57** (3), 97–111 (2021). https://doi.org/10.37190/ppmp/135749
19. F. Chen, F. Liu, L. Wang, J. Wang, Comparison of the preparation process of rare earth oxides from the water leaching solution of waste Nd-Fe-B magnets' sulfate roasting products. Processes **10**(11), 2310 (2022). https://doi.org/10.3390/pr10112310
20. Q. Liu, T. Tu, H. Guo, H. Cheng, X. Wang, High-efficiency simultaneous extraction of rare earth elements and iron from NdFeB waste by oxalic acid leaching. J. Rare Earths **39**(3), 323–330 (2021). https://doi.org/10.1016/j.jre.2020.04.020